Conceptual Study and Prototype Design of a Subsonic Transport UAV with VTOL Capabilities

A project present to
The Faculty of the Department of Aerospace Engineering
San Jose State University

in partial fulfillment of the requirements for the degree
Master of Science in Aerospace Engineering

By

Shayan Naiafi

May 2015

approved by

Dr. _____
Faculty Advisor

* Graduate Student of Aerospace Engineering, San Jose State University, shayan.najafi@sjsu.edu
† Assistant Professor, Aerospace Engineering, San Jose State University, kamran.turkoglu@sjsu.edu

American Institute of Aeronautics and Astronautics

Conceptual Study and Prototype Design
of a Subsonic Transport UAV with VTOL Capabilities

Shayan Najafi* and Kamran Turkoglu[†]

San Jose State University, San Jose, CA, 2014, United States

This study presents a conceptual design of an unmanned aerial vehicle (UAV) and develops controller algorithms for achieving specified closed-loop response characteristics on a transonic transport UAV with vertical takeoff and landing capabilities. The study will be done with data representing the aircraft at a steady symmetric flight condition, and will explore the option of using a Linear Quadratic Regulator (LQR) feedback system. Conceptual design and the prototype of the aircraft are conducted using conventional aircraft design techniques. The mission is to achieve low altitude cruise of 100 m/s with an effective range of 200 miles; furthermore the takeoff and landing are executed without the use of a runway. Initial system identification is conducted for a virtual model of the aircraft using vortex lattice methods through AVL[15]. The aircraft will use a combination of quad copter and airplane controls to take off and land autonomously from non-ideal locations.

Nomenclature

U	Axial Velocity
$\mathring{U}$	Axial Acceleration
Q	Pitch Rate
W	Normal Velocity
θ	Pitch Angle
h	Altitude hold
V	Lateral Velocity
P	Roll Rate
R	Yaw Rate
φ	Roll Angle
ψ	Yaw Angle
ζ	Rudder Deflection
ξ	Aileron Deflection
η	Elevator Deflection
$C_{L(max)}$	Maximum lift coefficient for specified airfoil
AOA	Angle of attack
C.G.	Center of gravity

I. Introduction

With the current state of modern UAVs, we have the ability to design quad rotor type vehicles capable of completely autonomous flights and mission objective completion. Additionally, methods described in Pfeifer[4] and Huang[5] provide pathways to constructing robust rotary wing aircraft capable of operation in both optimal and non-optimal conditions. The topic of quad copter controls has been widely covered by [6-10].

A comprehensive design methodology can also be found for control of traditional aircraft in subsonic flight regimes. Works by Ogata[11], Cook[12], Stevens and Lewis[13] and many more sources, provide recipes on closed loop designs for controlling longitudinal, lateral directional, and altitude hold states of traditional fixed wing systems.

Given the tools currently available, the design of a hybrid aircraft capable of initiating a mission in quad copter mode and moving on to achieve high subsonic cruise in aircraft mode is a conceivable option. Such an aircraft would be useful in any situation in which access to a remote location in a reasonably short amount of time is necessary, or highly desirable, and will be the main motivation of this study.

A successful completion of the mission will require an aircraft that can take-off from a single point, transition from hover to flight mode, cruise at 100m/s for a range of 100 miles, descend, receive payload, and return to base. The mission will be executed autonomously so that the user defines a destination and the aircraft uses GPS navigation to complete the mission with no other user input.

This paper aims to outline a pathway to creating such an aircraft from conceptual design to the production of the prototype with a special focus on the stability and controls challenges that are unique to VTOL vehicles. The initial design of the aircraft will be discussed along with the reasoning behind the configuration. The report will also over view the controls methods that can be used to stabilize the flight modes and discuss challenges yet to be addressed.

II. Aircraft Design

The initial aircraft design is completed following conventional methods outlined in Roskem[13] and Raymer[14]. In order to meet the mission's aircraft design parameters (i.e. aerodynamics, structure, etc.) the aircraft consists of a high wing, inverted V-tail design, for increases roll stability, a centrally mounted gas turbine for cruise, and four high thrust electric motors in an H configuration for the hover aspect (Figure 1). Although an electric propulsion system would be desirable due to cost and maintenance concerns, we ultimately find that a jet turbine is required to achieve the efficiency and range that are demanded by our mission. In order to reach the desired cruise speed, aerodynamics was heavily weighted in the overall design of the aircraft. We found that an aspect ratio close to 4 would allow us the necessary Oswald efficiency and structural weight to meet our mission, this consideration also allows enough space for the gas tank and electrical components. When deciding on a wing loading, the aircraft climb rate, structural weight, takeoff speed, overall lift, stability, and performance were taken into account. Because the aircraft's takeoff and landing are performed in hover mode, the takeoff speed and climb rate were not as heavily weighted. After completing a wing loading chart with the special considerations for the takeoff and climb rate limits, AVL[15] is used to consider configurations in different sectors of our envelope.
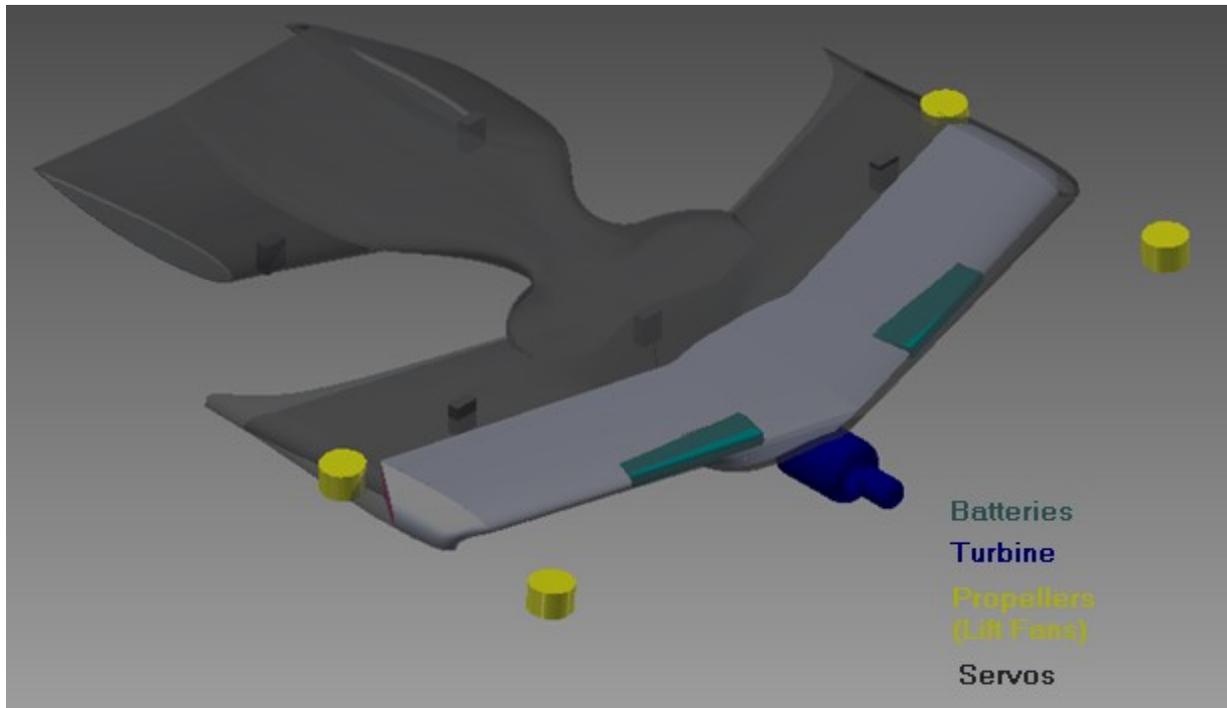
Figure 1. General configuration of aircraft.

During the preliminary design, a vortex lattice representation of the aircraft was created using AVL, as shown in Figure 2, and the control surfaces were sized to trim the aircraft and provide adequate roll and yaw authority. During the iterations we found that it was necessary to move the C.G. and aerodynamic center to ensure that the aircraft would remain statically and dynamically stable without control augmentation. This is done to supply enough static stability margin in the open loop control dynamics and provide a level of safety to the system. A traditional tail was chosen over a canard configurations primarily because it would help to achieve longitudinal stability, the vertical stabilizers were pointed downward to eliminate the need for lengthy landing gears in the aft section. Further studies through AVL show that the size and position of the lifting surfaces have a much greater effect on stability than the camber of the airfoils. The rough sizing of the main wing was done to ensure enough lift during all flight conditions and near zero AOA during cruise. Then, the geometries of the lifting surfaces were fine-tuned with AVL to statically stabilize the aircraft. Starting with a database of high L/D ratio airfoils in our cruise Reynolds range, we imported combinations of camber profiles into AVL and found a viable array of combinations that would allow our aircraft to achieve adequate $C_{L(max)}$ during takeoff, cruise at an AOA with minimum drag, and have enough authority to trim and maneuver. It is important to note that the hinge line for each of the control surfaces required an additional iterative review to meet performance specifications. Because of the reason that vortex lattice models have limited accuracy in calculating drag, we were also required to run CFD studies for the final designs to improve the accuracy of our results. The CFD results are later verified though wind-tunnel testing. When the final body design was selected we found that the

aerodynamic characteristics allow us to decrease thrust required for our design, and this in return allowed us to utilize a smaller turbine. With the decrease in power plant weight, we were able to decrease the size of the lift fans, structure, batteries, and gas tank which resulted in a further weight reduction; this cycle continued until a convergence point was reached.

Other considerations for practicality, thermal effects, flight regime, and stall characteristics also had to be made. An alpha sweep of the CFD model suggested a tip stall tendency at high AOA which was rectified by the implementation of aerodynamic twist in the span wise wing design. Geometric twist was also considered for this problem, but it would overly complicate the design and mounting of the outboard lift fans. We found that a decrease in camber of 2 degrees starting at 45% span was enough to rectify the problem. A series of test bed experiments showed that the aircraft (jet turbine configuration) experiences a drift in C.G. during flight. Because we know that quad copter controls are susceptible to changes in C.G., it is important to ensure that the lift fans can provide enough thrust so that the controls can compensate for the full and empty configurations. A simple force balance model provided us the theoretical maximum lift needed when the aircraft has no fuel (C.G. forward limit), and a 10% safety factor was added to this value. Additionally a sweep of 16 degrees was added to the main wing to ensure that the front lift fans were not obstructed by the main wing.

The majority of the control theory related to the hover mode of the aircraft will be derived using existing work on common quad-copters. The 6 degree of freedom coupled equations of motion shown in Huang[5] will be used to create a state space representation of our model with our specific inertial and aerodynamic values added in.
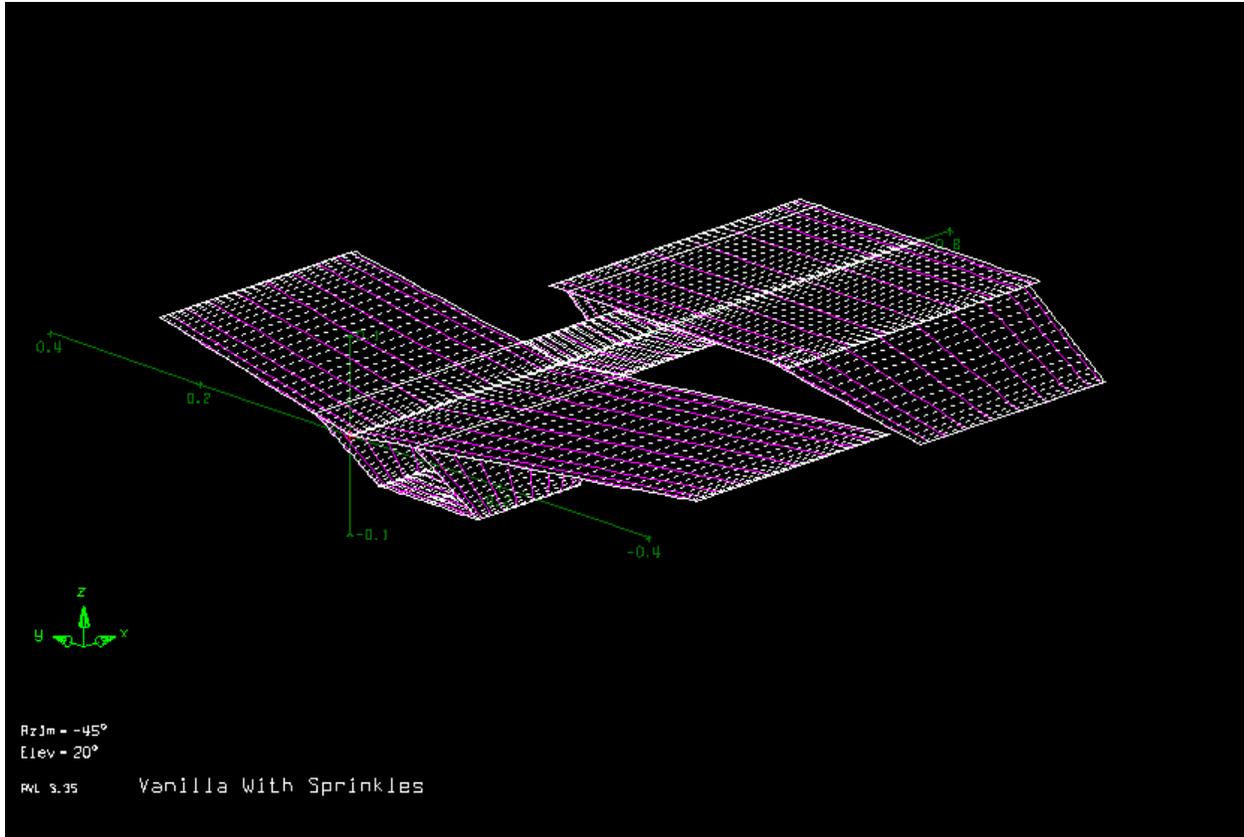
Figure 2. Vortex lattice approximation of UAV model.

We can create a controller for the hover mode and blend the control signal to the lift fans with the inputs to the turbine, and lifting surface servos, to create a blended controller for the hover to cruise and cruise to hover sections of our mission. Introducing sweep to the wing is also a preemptive consideration for compressibility effects that will need to be addressed if the aircraft is to cruise at transonic speeds as a part of future works.

Identification of the system was also performed using AVL. The longitudinal (U,Q,W, θ, h) and lateral directional (V,P,R, φ, ψ) states are obtained through inputting the moment of inertia, mass, and executing an Eigen mode analysis for cruise conditions.

III. Open Loop Dynamics

The pole locations for our system in AVL give us a clear view of the dynamic response (as provided in Figure 3). Here, using an iterative process in AVL, the C.G. and aerodynamic center locations are finalized for the final design stage.
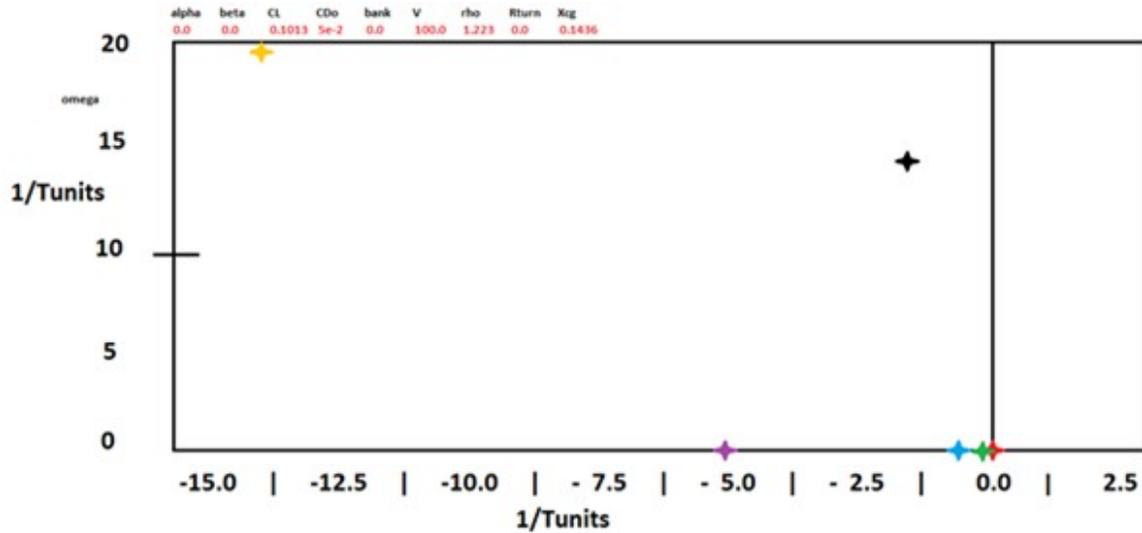
Figure 3. Final dynamic mode locations.

Next is the investigation of the open loop response, which will help us to verify our findings in AVL. Open loop response characteristics are shown in Figure 4.
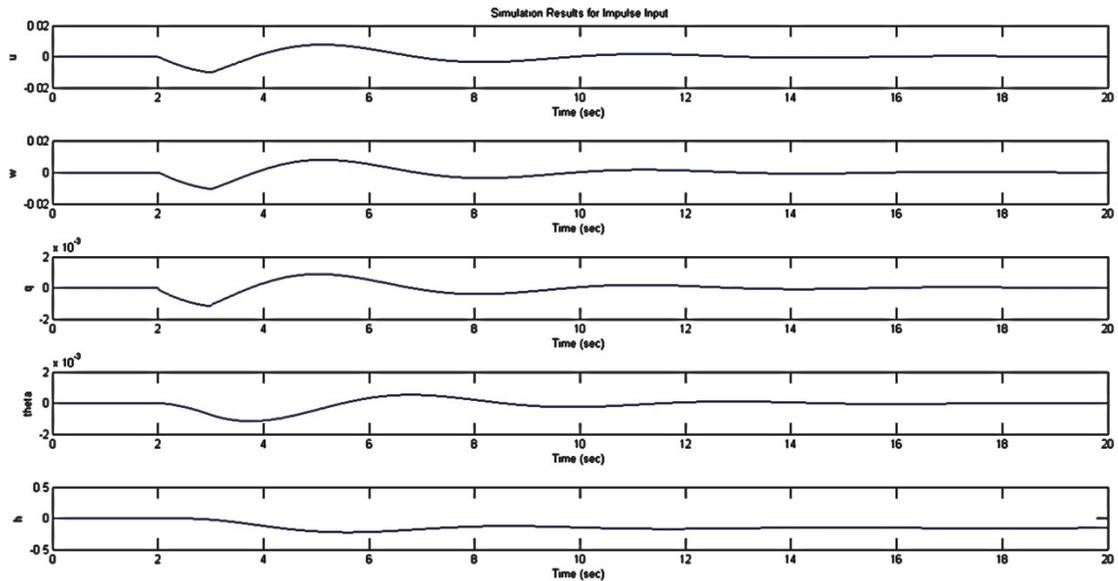

Figure 4. Open-loop response of longitudinal dynamics.

As expected, the time response function in our AVL model shows that the overall system is stable and reaches a final steady state value. The final design of the aircraft was affected in three ways: the C.G. and aerodynamic center were adjusted, the aircraft was also found to lack elevator authority to trim and stabilize, so the V tail was angled up an additional 5 degrees. This change

American Institute of Aeronautics and Astronautics

resulted in decreased directional control, but the changes are within acceptable limits. Finally the camber on the aft airfoil was changed to compensate for the changes to the rudder. By augmenting the rear airfoil we obtained a 3% decrease in drag which proved to be beneficial. The hinge points for the control surfaces were set through an iterative process which took controls considerations and servo limitations into account.

IV. Feedback Control System Design

Linear Quadratic Regulator (LQR) based controllers are a form of optimal control authority commonly used in aircraft to achieve the optimal performance for the least amount of control effort. For this study, a linear quadratic regulator (LQR) was designed with the following goals: overshoot less than two percent, settling time less than one second, steady state error less than one percent, and control effort less than five Newtons.

The observability and controllability matrices were both full rank, which ensures that the system is observable and controllable. The first controller design is an LQR controller with the system defined by Eqs. (1) and (2), and state feedback defined by (3).

$$\dot{x} = Ax + Bu \tag{1}$$

$$y = Cx + Du \tag{2}$$

where

$$u = -K_{lqr} x \tag{3}$$

A first order actuator model (4) was used to simulate actuator dynamics to account for actuation between control input and control surface deflection.

$$TF_{actuator} = \frac{15}{s + 15} \tag{4}$$

$$Q = gain * C'C \tag{5}$$

Because the MATLAB "lqr" command does generates the best response without concern to the value of the steady-state, a pre-filter gain was added before the actuator to reduce steady state error. The closed loop system with the addition of the pre-filter gain is given by (6) for a given reference signal.

$$\dot{x} = (A - B K_{lqr}) x + B K_{pre} R \tag{6}$$

Taking the Laplace of equation 6.6 and re-arranging terms resulted in (**7**).

$$x = \left(SI - A + B K_{lqr} \right)^{-1} B K_{pre} R \tag{7}$$

By setting the state equal to the reference signal and utilizing the final value theorem, the term containing s goes to zero and the pre-filter gain is determined by (8).

$$K_{pre} = -\left(\left(A - B K_{lqr} \right)^{-1} B \right)^{-1} \tag{8}$$

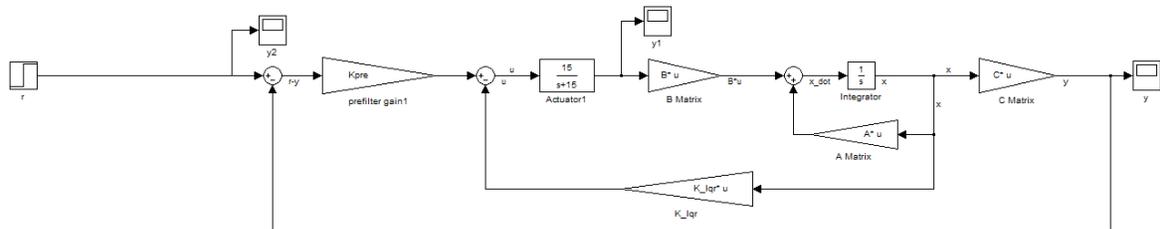The Q and R matrices were initially weighted equally A MATLAB script was used in combination with a Simulink model, Figure 5, to evaluate the time history response of the system.

Figure 5. Nominal linear quadratic regulator controller with a step input.

The tuning process for this system is now dependent on the weighting of Q (as given in Eq.(5)) and R (which is usually denoted with unity). By setting/adjusting weights, a tradeoff is achieved between transient and steady-state responses of the system dynamics.

At this point, due to the nature of full-state feedback algorithms, in order to correct for the off-set in the desired steady state value, it was necessary to introduce a pre filter gain which in effect created a partially-augmented LQR system. With this system we are able to set the desired values for Q and R to achieve our given characteristics.
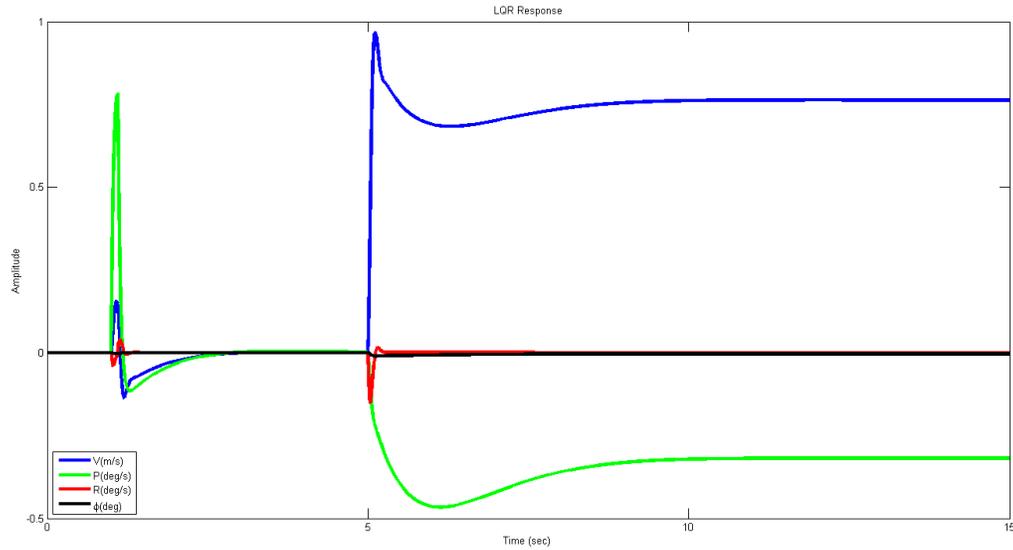
Figure 6. Lateral directional responses to impulse and step inputs.

Looking at the system as a whole in Figure 6 we can see the aircraft's response to an impulse in the rudder followed by a step input to the ailerons. Variation of the Q and R matrixes allows us to compromise between the responses of each state until a satisfactory median is reached.
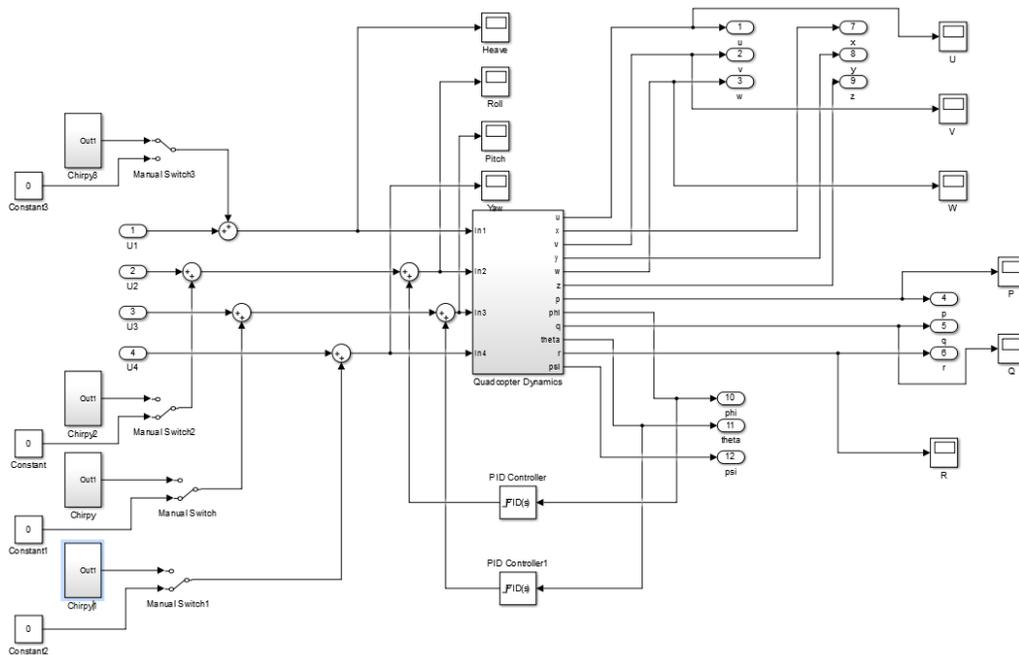
V. Build and Testing

Figure 7. MATLAB Simulink setup for quad-copter.

With a viable design completed for the feedback controller we can move on to the design

of the quad-copter used in our hover regime. A Simulink model, as shown in Figure 7, was built to represent the responses from a generic quad-copter with our specific weight and moment of inertia properties. The simulation block includes the basic equations of motion for quad-copters as well as aerodynamic estimates calculated in a similar manner to Bristeau[18]. Through the use of this simulation we are able to build a rudimentary PID controller which will allow the quad-copter test bed to fly well enough perform system identification. The specific values and feedback loops used are listed in Table 1.

Table 1. PID Controller Values for Quadcopter Configuration

State	P Value	I Value	D Value
Roll	4.57	0	0
Pitch	4.57	0	0
Yaw	4.55	0	0
Roll Rate	0.163	0.100	0.0035
Pitch Rate	0.163	0.100	0.0035
Yaw Rate	0.225	0.02	0
Throttle	0.077	1.65	0
Throttle Rate	4.05	0	0

Extensive work in the field of auto-gyro stabilization and control has been done by the open source community and was a valuable asset in this project. After building the Simulink model of our design, test flights were conducted on a prototype test bed (shown in Figure 8) to
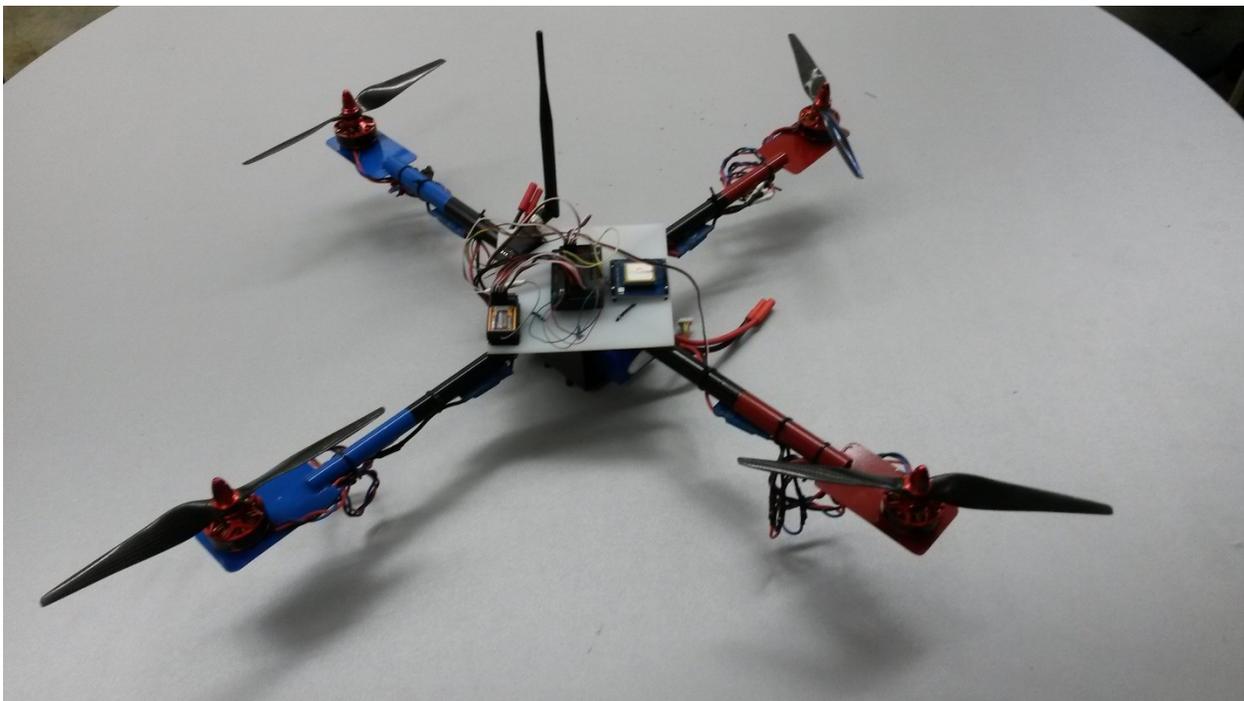

Figure 8. Quad-copter test bed.

obtain data for control system analysis. As with the airplane, the quad-copter is designed to have response characteristics that are satisfactory for the mission; however, tuning the gains on the quad-copter is more discretionary because it was set to parameters that seem visually acceptable during flight testing and shakedown. Stricter criterion will be imposed later when the aircraft has successfully flown its mission.

The coding and controller implementation for the both the quad-copter and the airplane modes was done by augmenting available open source code to utilize LQR methodology and transition between hover and flight phases by gain scheduling to airspeed, this process is discussed further in section VI. The quad-copter used to design the hover mode for the final prototype is laid out with a very conventional design.

In this study, the entire project uses an Arduino Mega open source platform CPU, 433 MHz 3DR telemetry module, Spektrum DX8 transmitter and receiver, MaxSonar ultra sonic sensor, and uBlox NEO6M compass and GPS module. The mentioned items are used to build the controllers for both the quad-copter and airplane test beds as well as the final product.

At this stage in the manufacturing process, open source code was used to inherit a ground station, data acquisition, waypoint management and flight mode switching. The quad copter's original altitude sensing was done by barometric measurements; however, during testing it was found that the quad-copter would experience significant oscillations in altitude due to vibrational noise from the electric motors.

In order to remedy the problem, all of the sensors had to be fitted with a damping plate to filter out high frequency noise. In addition, an ultra-sonic sensor was substituted for the barometer to altitude measurements. The setup allowed test data to be transmitted in real time, so stick inputs and corresponding Euler angles (θ,ψ,ϕ), angular rates (P,Q,R) and linear accelerations, as well as h and record time were logged for bare airframe system identification. System identification of the existing test-bed is currently an ongoing research effort, and obtained results will be reported in another study.

Before testing can begin however, the airplane portion itself is constructed using carbon fiber to allow for a light airframe that can support all of the necessary flight and hover loads. The airframe itself consists of an aramid honeycomb core sandwiched by two layers of graphite fiber Figure 9. This allows the internals of the airframe to remain hollow for actuator components, fuel and the power plant.
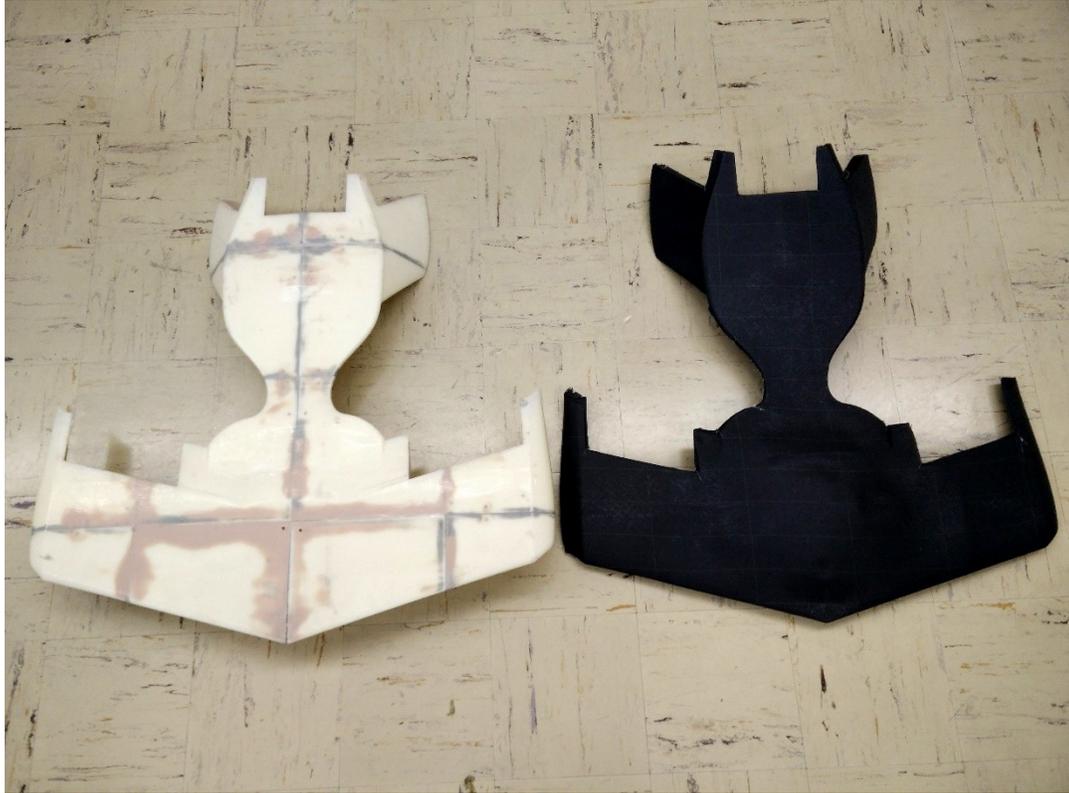
Figure 9. Mold and airframe top section

VIII. Technical Issues

Beyond the theoretical challenges that were introduced in this set up, there were a number of hurdles involved with the manufacturing and implementation of the configuration. The voltage regulation system on the micro controller had to be wired to insure that the proper voltage was supplied to both the motherboard and the daughter board. The power was initially supplied to each of the boards through the power and signal wires from the speed controllers. It was later discovered that dedicating a power supply to each board would result in a critical failure. Although all of the speed controllers are designed to supply the same voltage, there are minute differences in actual voltage supplied by each controller, which causes synchronization problems between the boards. This problem causes a random dip in the first motor which occasionally results in a crash. The problem was solved by adding a parallel bus which was powered by a single source and gave power to the mother board and all of the daughter boards, this way all of the components receive the exact same voltage eliminating the discrepancies.

Other complications were apparent in the power electronics. The controller is powered by a power module which sits in line with the number 1 motor and draws power in parallel. The existence of this circuit would cause the number 1 motor to overheat as shown in Figure 10.
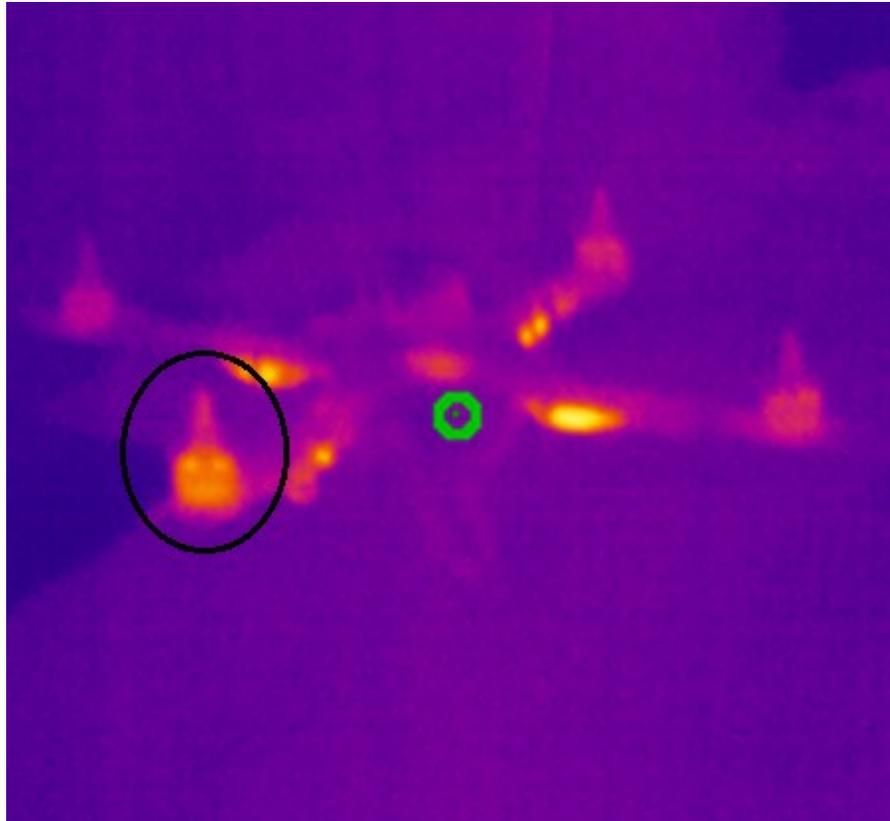
Figure 10. Infrared view of stress test (Erroneous Motor Circled).

A solution was found by routing power to the controller directly through the speed controller and eliminating the power regulator from the system.

IX. CFD Confirmation and Flight Results

Although structural data acquisition models, through strain gauge measurements, could not be utilized due to time constraints; use of onboard accelerometers and gyros allowed us to make simple confirmations for the CFD results by comparing predicted climb rates and maximum speeds to test results. The results show that all the CFD results (Figure 10) are within a 6% accuracy window.
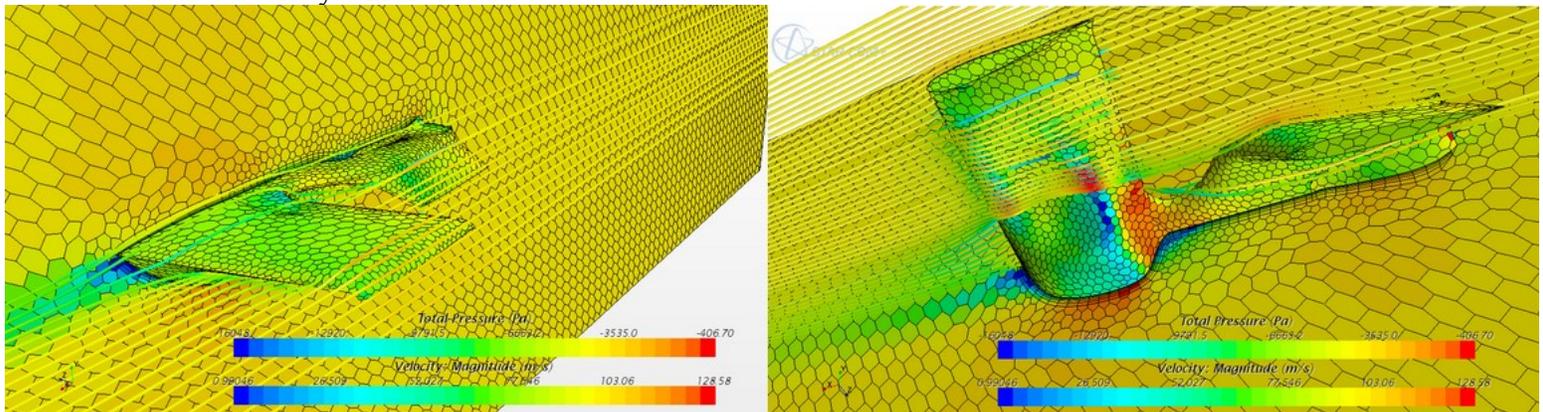
Figure 10. CFD Simulation for 0º AOA

Figure 10 shows the aircraft at cruise speed. The total pressure is depicted on the skin of the aircraft and ranges from -160 Pa to 407 Pa from a reference pressure of 101325 Pa. This depiction is useful for identifying aerodynamic inefficiencies. It is important to note that the jet stream from the power plant is not modeled in this simulation. The velocity profile is shown through the X-Z plane of the aircraft. Velocity streamlines are also seeded at the approximate location of the leading edge. The information gathered from the CFD simulations was used to augment the profile of the aircraft to improve aerodynamic flight characteristics before the flight test model was built.

Identification of the state space model for electrical cruise conditions was done with a series of chirp maneuvers to capture all of the system dynamics. A sample of the acquired input and output flight data is shown in Figure 11.
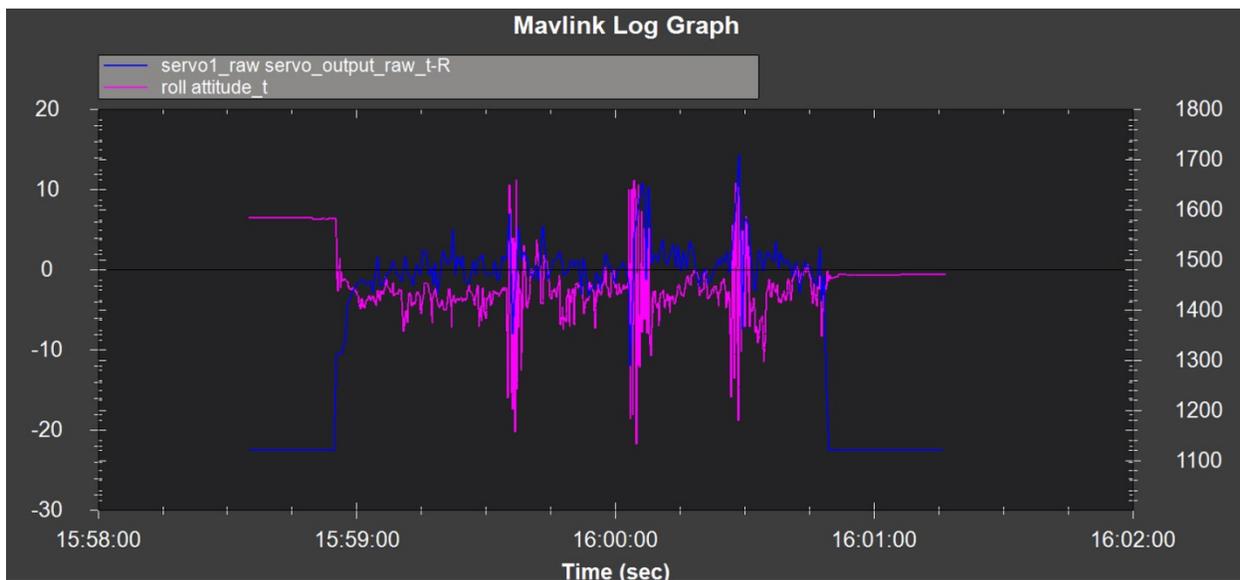

Figure 11. Input vs. Output Data for Roll Chirp

The chirp data for the tested aircraft (Figure 12) is used to identify the aircraft's state space model (Table 2) for cruise conditions with no external payloads using frequency domain identification methods.
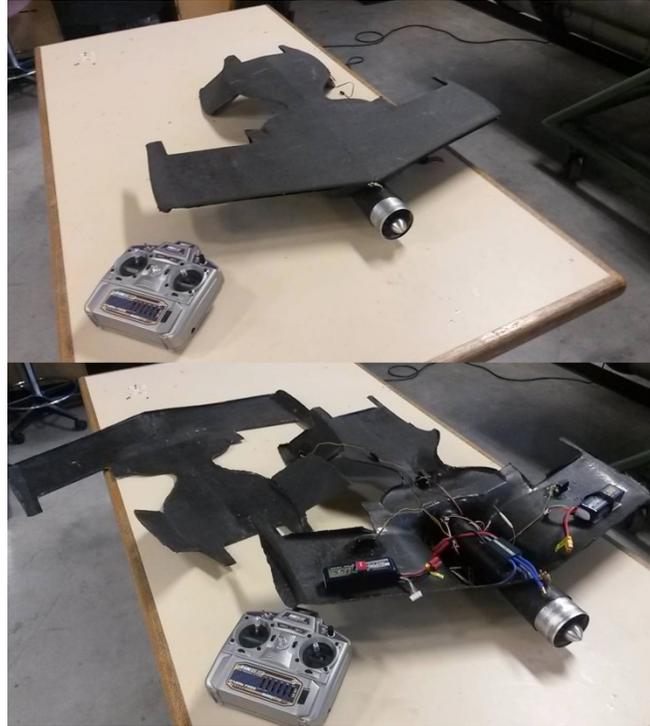
Figure 12. Aircraft Structure and Internals
Table 2. State Space Model for Aircraft

		u	w	q	theta			elevator	
d/dt	u	-0.311	-0.021	-0.032	-9.810			0.000	
	w	0.368	-8.788	47.681	0.000			-1.440	
	q	5.562	-4.305	-6.635	0.000			-8.911	
	theta	0.000	0.000	1.000	0.000			0.000	
		v	p	r	phi	psi		aileron	rudder
d/dt	v	-0.790	0.037	-49.744	9.810	0.000		0.142	0.000
	p	1.093	-2.717	-0.749	0.000	0.000		6.442	-0.334
	r	1.178	-0.003	-0.957	0.000	0.000		-0.511	-2.342
	phi	0.000	1.000	0.000	0.000	0.000		0.000	0.000
	psi	0.000	0.000	1.000	0.000	0.000		0.000	0.000

The acquired state space model has an associated cost function ranking below 100 which shows that there is acceptable correlation between the flight data and the respective A and B matrices. During the state space derivation, known parameters are substituted in for free variables to constrain the state space model. For example, known C.G. position, moments of

inertia and symmetry in the X-Z plane allow us to explicitly enter or eliminate many off- axis and geometry specific values.

X. Conclusion and Future Works

This report provides a viable conceptual and physical design of a subsonic transport aircraft with VTOL capabilities. To meet the mission's aircraft design parameters (i.e. aerodynamics, structure, etc.) the aircraft consists of a high wing, inverted V-tail design, for increases roll stability, a centrally mounted power plant for cruise, and four high thrust electric motors in an H configuration for the hover aspect. Theoretical identification of the open-loop system was also performed using AVL. The longitudinal (U,Q,W, θ, h) and lateral directional (V,P,R, φ, ψ) states are obtained through inputting the moment of inertia, mass, and executing an Eigen mode analysis for cruise conditions. After building test beds and identifying plant models, our findings show that by using a LQR control scheme and tuning our desired values for acceptable overshoot and transience response, a nominal controller can be designed to provide response for all of the expected flight modes and states. In future works, benefits in controls, structure, and aerodynamic aspects would also be realized with the implementation of thrust vectoring on the main thruster to minimize or eliminate the need for propeller driven quad motors. Further studies that can be conducted on the test bed will include gain scheduling the respective plants, and investigation into thrust vectoring and pivoting the main engine to illuminate the need of propellers.

Acknowledgments

References

[1] J.B. Hoagg and D.S. Bernstine, "Non-Minimum Phase Zeros: Much to do about Nothing," IEEE Trans. Automat. Conr., vol.16, pp.45-57, 2007.

[2] Athans, Michael; Castanon, David; Dunn, Keh-Ping; Greene, Christopher; Lee, Wing; Sandell jr, Nils; Willsky, Alan; *The Stochastic Control of the F-8C Aircraft Using a Multiple Model Adaptive Control (MMAC) method – Part 1: Equilibrium Flight*, IEEE Transactions On Aautomatic Control, VOL AC-22, NO. 5, OCTOBER 1977

[3] Greene, Christopher*, Application of the Multiple Model Adaptive Control Method to the Control of the Lateral Dynamics of an Aircraft, Masters Dissertation*, University of Colorado, 1973

[4] Pfeifer, E.; Kassab, F., *Dynamic Feedback Controller of an Unmanned Aerial Vehicle,* Robotics Symposium and Latin American Robotics Symposium (SBR-LARS), 2012 Brazilian , vol., no., pp.261,266, 16-19 Oct. 2012
doi: 10.1109/SBR-LARS.2012.49

[5] Haomiao Huang; Hoffmann, G.M.; Waslander, S.L.; Tomlin, C.J., *Aerodynamics and control of autonomous quadrotor helicopters in aggressive maneuvering,* Robotics and Automation, 2009. ICRA '09. IEEE International Conference on , vol., no., pp.3277,3282, 12-17 May 2009

[6] G. Hoffmann, D. G. Rajnarayan, S. L. Waslander, D. Dostal, J. S. Jang, and C. J. Tomlin, *The stanford testbed of autonomous rotorcraft for multi agent control (STARMAC),"* in Proceedings of the 23rd Digital Avionics Systems Conference, (Salt Lake City, UT), pp. 12.E.4/1-10, November 2004.

[7] S. Bouabdallah, P. Murrieri, and R. Siegwart, *Towards autonomous indoor micro VTOL,* Autonomous Robots, vol.18, pp. 171-183, March 2005.

[8] E. B. Nice, *Design of a four rotor hovering vehicle,* Master's thesis, Cornell University, 2004.

[9] P. Pounds, R. Mahony, and P. Corke, *Modeling and control of a quad-rotor robot,* in Proceedings of the Australasian Conference on Robotics and Automation, (Auckland, New Zealand), 2006.

[10] E. Altuǧ, J. P. Ostrowski, and C. J. Taylor, *Quadrotor control using dual camera visual feedback,* in Proceedings of the IEEE International Conference on Robotics and Automation, (Taipei, Taiwan), pp. 4294-4299, Sept 2003.

[11] Ogata, K., Modern Control Engineering, 5th ed., Englewood Cliffs, New Jersey, 1970

[12] Cook, M. V. Flight dynamics principles, 2nd ed, Amsterdam, Elsevier/Butterworth-Heinemann, 2007

[13] Roskam, J., Airplane design, Ottawa, Kansas, Roskam Aviation and Engineering Corp.,1985

[14] Raymer, D. P., Aircraft design: a conceptual approach, Washington, D.C., American Institute of Aeronautics and Astronautics, 1989

[15] Drela, M., Youngren H, AVL Aerodynamic Analysis Trim Calculations Dynamic Stability Analysis Aircraft Configuration development, Boston, MA, Massachusetts Institute of Technology, 2014

[16] Stevens, B. L. and Lewis, F. L., Aircraft Control and Simulation, Wiley, 2003

[17] Tischler, M. B., and Kemple, R. K., *Aircraft and Rotorcraft System Identification*, 2nd ed., AIAA Educational Series, AIAA, Virginia, 2012.

[18] Bristeau, P., Martin, P., Salaün, E., Petit, N., "The role of propeller Aerodynamics in the Model of a Quadrotor UAV," *European Control Conference,* Budapest, 2009, pp. 683-688.